MATHEMATICAL ENGINEERING TECHNICAL REPORTS

Exact Performance Analysis of MIMO Zero-Forcing Detection for Transmit-Correlated Rician-Rayleigh Fading

Constantin SIRITEANU, Steven D. BLOSTEIN,
Akimichi TAKEMURA, Hyundong SHIN,
Shahram YOUSEFI

METR 2013–07 May 2013

DEPARTMENT OF MATHEMATICAL INFORMATICS
GRADUATE SCHOOL OF INFORMATION SCIENCE AND TECHNOLOGY
THE UNIVERSITY OF TOKYO
BUNKYO-KU, TOKYO 113-8656, JAPAN

WWW page: http://www.keisu.t.u-tokyo.ac.jp/research/techrep/index.html

Exact Performance Analysis of MIMO Zero-Forcing Detection for Transmit-Correlated Rician–Rayleigh Fading

Constantin Siriteanu, Steven D. Blostein, Akimichi Takemura, Hyundong Shin, Shahram Yousefi

Abstract

This paper reveals a previously-unknown infinite linear combination of Gamma distributions with simple coefficients for the symbol-detection signal-to-noise ratio (SNR) in multiple-input/multiple-output (MIMO) communications employing spatial multiplexing and zero-forcing detection (ZF), whereby the intended (detected) and interfering symbol streams experience correlated Rician and Rayleigh fading, respectively. Our derivation of the exact moment generating function (m.g.f.) of the ZF SNR for the Rician-fading stream bypasses the noncentral-Wishart distribution, whose intractability has required previously approximation with a central-Wishart distribution of equal mean. We also express exactly the ZF SNR moments and probability density function, as well as the ZF average error probability, outage probability, and ergodic capacity. Numerical results from analysis and Monte Carlo simulations confirm the accuracy of our new expressions and reveal that the symbol-detection performance for the Rician-fading stream is: 1) unaffected by the 'direction' of the channel-vector mean, 2) unaffected by transmit-correlation, at realistic K values (unlike for Rayleigh–Rayleigh fading), 3) seriously degraded by Rayleigh-fading interference even for large K, which is of concern in heterogeneous networks.

Index Terms

Azimuth spread, K-factor, Gamma distribution, MIMO, Rayleigh and Rician (Ricean) fading, transmit correlation, Wishart distribution, zero-forcing.

C. Siriteanu and A. Takemura are with the Department of Mathematical Informatics, Graduate School of Information Science and Technology, University of Tokyo, Japan, and the Japan Science and Technology Agency, CREST.

S. D. Blostein and S. Yousefi are with the Department of Electrical and Computer Engineering, Queen's University, Canada.

H. Shin is with the Department of Electronics and Radio Engineering, Kyung Hee University, South Korea.

I. INTRODUCTION

A. Background, Motivation, and Assumptions

Multiple-input/multiple-output (MIMO) wireless communication theory, simulation, and implementation have demonstrated that substantial performance gains are possible by suitable signal processing at the transmit and receive antennas [1] [2] [3] [4] [5] [6] [7] [8]. In single-user (SU) MIMO systems, a multi-antenna base-station communicates in each time–frequency slot with a sole mobile station that uses multiple antennas. On the other hand, in multi-user (MU) MIMO systems, the multi-antenna base-station communicates with several mobile stations (i.e., spatial multiple access [4]), with each employing one or several antennas. Spatial multiplexing, whereby streams of symbols are transmitted from each antenna, enhances data rate [4].

Although SU and MU MIMO spatial multiplexing have already been standardized in modern wireless systems [5] [9] [10] [11], the effects of realistic propagation features, e.g., a channel matrix with nonzero mean and correlation, on performance are not yet fully understood even for low-complexity linear symbol-detection methods, e.g., zero-forcing detection (ZF) and minimum mean-square error detection (MMSE) [12]. The former cancels interstream interference but may enhance the noise, whereas the latter balances interference and noise but requires knowledge of the noise variance[1]. Whereas MMSE is often adopted in baseline performance evaluations of MIMO [5] [10] [11], it is also difficult to analyze [14] [15] [13] [16] [17] [18]. Thus, we focus herein on analyzing ZF, and leave MMSE for future work.

Conventionally, MIMO ZF performance has been studied for simple channel models, e.g., Rayleigh fading and zero spatial correlation [19] [20] [21] [22] [23]. However, the state-of-the-art WINNER II channel model [24] [25] has revealed that measured fading is characterized by the Rician distribution. Then, the mean and correlation of the complex Gaussian fading gains are determined by the scenario-dependent values of the K-factor and azimuth spread (AS) [26]. The AS represents the second central moment of the power azimuth spectrum, which is typically assumed to be of Laplacian type, e.g., in WINNER II. Other empirically-based closed-form expressions that accurately relate the power azimuth spectrum to important scenario parameters have also been proposed — see [27] and references therein.

[1]Note that, since the streams are detected independently, by regarding one stream as intended and the remaining as interfering, MMSE and optimum combining are equivalent [13, Remark, p. 2349].

In addition, only approximate analyses of ZF are available when all streams encounter Rician fading, with [26] [28] [29] [30] exploiting an approximation of the intractable noncentral-Wishart matrix distribution with a central-Wishart matrix distribution of equal mean, as proposed in [31]. Thus, Siriteanu *et al.* [26] derived for MIMO ZF an approximate average error probability (AEP) expression from the moment generating function (m.g.f.) of the Gamma-distributed approximation of the symbol-detection signal-to-noise ratio (SNR). However, as explained in [26] and later in this paper, this approximation is unreliable. Therefore, our motivation herein is to provide the first exact (i.e., reliable) ZF analysis, by circumventing the Wishart distribution approximation.

We assume zero receive-correlation, which is realistic for widely-spaced receive-antennas immersed in rich scattering. This assumption also helps ensure analytical tractability [19] [20]. On the other hand, nonzero transmit-correlation is allowed, which is relevant for: 1) SU MIMO with insufficient transmit-antenna spacing or narrow transmit-AS, and 2) MU MIMO with streams from different mobile stations experiencing correlated fading [24]. Nevertheless, we shall find that the transmit-correlation has little effect on ZF performance for realistic Rician fading.

We also consider the following realistic fading model: only the intended stream (i.e., detected stream, whose symbol-detection performance is analyzed and simulated herein) encounters Rician fading, whereas the unintended (i.e., interfering) streams encounter Rayleigh fading. This scenario is referred to herein as Rician–Rayleigh fading[2]. Analyses of MIMO optimum combining and maximal ratio combining (MRC) have appeared in [13] [15] [32] [33] based on this Rician–Rayleigh fading model, which was supported there by the view that intended and interfering streams propagate as line-of-sight and non-line-of-sight, respectively, in microcellular and indoor environments. The Rician–Rayleigh assumption is also relevant for heterogeneous network [11], as envisioned in [34] [35] [36] based on the following standard femtocell–macrocell interference scenarios proposed in [37] [38] [39] [40]: 1) intended stream from an indoor femtocell user and interfering streams from outdoor mobile macrocell users reach multi-antenna femtocell base-station; 2) intended stream from the femtocell base-station and interfering streams from macrocell base-stations reach the multi-antenna femtocell user-station.

Note that ZF is applicable only when the number of receive antennas N_{R} is not smaller than the number of transmitted streams N_{T}, i.e., $N_{\mathrm{R}} \geq N_{\mathrm{T}}$, so that we can compute a crucial matrix

[2]Or, simply, as *Rician fading*. On the other hand, Rayleigh–Rayleigh fading is also referred to herein as *Rayleigh fading*.

inverse that enters the ZF definition [2, p. 153]. But, although our derivations herein require the assumption $N_{\mathrm{R}} \geq N_{\mathrm{T}}$, our results also apply for $N_{\mathrm{R}} < N_{\mathrm{T}}$ if the contributions from $N_{\mathrm{T}} - N_{\mathrm{R}}$ interferers can be compounded with the receiver noise into a zero-mean white Gaussian vector.

B. Previous Work. Contributions

For transmit-correlated Rayleigh–Rayleigh fading, Gore *et al.* [19] showed that the ZF SNR is Gamma distributed by using the central-Wishart distribution of the matrix that appears in the SNR expression commonly used in ZF analyses [19, Eq. (5)]. This matrix has a noncentral-Wishart distribution when any of the streams encounter Rician fading, rendering intractable the derivation of the exact SNR distribution as in [19]. The approximation with a central-Wishart-distributed matrix of equal mean employed in [28] [29] [30] has been found fairly reliable for the case of a rank-one channel-matrix mean that is formed as an outer-product of the transmit and receive array steering vectors [26]. Although the channel-matrix mean is also rank-one for Rician–Rayleigh fading, our numerical results herein reveal that the Wishart distribution approximation is then unreliable. Thus, we have sought to bypass the Wishart distribution by recasting the ZF SNR in a more tractable form than the conventional ratio form [19, Eq. (5)].

Thus, we have found that Kang and Alouini expressed the signal-to-interference ratio for MIMO optimum combining as a Hermitian form with separated intended and interfering contributions, in [33, Eq. (7)], for receive-correlated Rician–Rayleigh fading in an interference-limited scenario (i.e., $N_{\mathrm{R}} < N_{\mathrm{T}}$), and derived its probability density function (p.d.f.) by using James' result [33, Theorem 1] on the distribution of a Hermitian-like form. For ZF, Kiessling and Speidel were the first to cleverly recast the SNR for transmit-correlated Rayleigh–Rayleigh fading as the Hermitian form in [20, Eq. (7)], which conveniently separates, similarly but not exactly as for optimum combining in [33, Eq. (7)], the intended and interfering contributions: the vector accounts for the intended channel vector, whereas the matrix, which is idempotent[3], accounts for the interfering channel vectors. This Hermitian-form expression for the ZF SNR is little-known compared to [19, Eq. (5)], but has appeared in [17, Eq. (15)] [41, Eq. (38)].

Now, in general, m.g.f. derivation for a Hermitian form in a random vector and a random matrix requires tedious averaging over both. Averaging over the random matrix requires averaging over

[3]Matrix $\mathbf{A}$ is *idempotent* if $\mathbf{A}^2 = \mathbf{A}$. Its eigenvalue matrix is then idempotent. Thus, its eigenvalues are either 0 or 1.

its eigenvalues and eigenvectors. Such a derivation is illustrated by McKay *et al.* in [15], and the resulting expression of the m.g.f. for the signal-to-interference-plus-noise of optimum combining in (uncorrelated) Rician–Rayleigh is very complicated [15, Eqs. (13)-(19)]. Basnayaka *et al.* [41] followed the same approach for ZF in Rayleigh–Rayleigh fading and a single interferer, but produced an m.g.f. expression that cannot be used for performance-measure derivations [41, Eq. (41)]. On the other hand, by explicitly accounting for the fact that the eigenvalues of the random idempotent matrix that enters the ZF SNR Hermitian form are deterministic and take values zero and one, Kiessling and Speidel [20] easily rederived for the ZF SNR the Gamma distribution which was originally found by using the Wishart distribution by Gore *et al.* in [19, Eqs. (9)].

Therefore, as in [20], but for transmit-correlated Rician–Rayleigh fading, we recast herein the ZF SNR as a Hermitian form in a Gaussian vector and an idempotent matrix. The exact expression for the m.g.f. of this Hermitian form is then derived by first conditioning on, and then averaging over, the idempotent matrix (i.e., over its eigenvectors). This m.g.f. expression yields new and relatively simple expressions for the MIMO ZF SNR moments, p.d.f., and cumulative distribution function (c.d.f.). From them, we express exactly, for the first time for Rician–Rayleigh fading, the ZF AEP, outage probability, and capacity. Finally, we use these expressions to investigate and reveal interesting effects on performance of the interference, K, and AS.

C. Notation

Scalars, vectors, and matrices are represented with lowercase italics, lowercase boldface, and uppercase boldface, respectively, e.g., h, $\mathbf{h}$, and $\mathbf{H}$; $\mathbf{h} \sim \mathcal{N}_\mathrm{c}(\mathbf{h}_\mathrm{d}, \mathbf{R}_\mathbf{h})$ indicates that $\mathbf{h}$ is a complex-valued circularly-symmetric Gaussian random vector [2, p. 39] with mean (i.e., deterministic component) $\mathbf{h}_\mathrm{d}$ and covariance $\mathbf{R}_\mathbf{h}$; subscripts $\cdot_\mathrm{d}$ and $\cdot_\mathrm{r}$ identify, respectively, the deterministic and random components of a scalar, vector, or matrix; subscript $\cdot_\mathrm{n}$ indicates a normalized variable; $i = 1 : N$ stands for the enumeration $i = 1, 2, \ldots N$; superscripts $\cdot^\mathcal{T}$ and $\cdot^\mathcal{H}$ stand for transpose and Hermitian (i.e., complex-conjugate) transpose; $[\cdot]_{i,j}$ indicates the i, jth element of a matrix; $\|\mathbf{H}\|^2 = \sum_i^{N_\mathrm{R}} \sum_j^{N_\mathrm{T}} |[\mathbf{H}]_{i,j}|^2 = \mathrm{tr}(\mathbf{H}^\mathcal{H}\mathbf{H})$ is the squared Frobenius norm of $\mathbf{H}$; r represents $\mathrm{rank}(\mathbf{H}_\mathrm{d})$; $\mathbb{E}\{\cdot\}$ denotes statistical average; $\simeq$ indicates that the random variables on the left and right have the same distribution; $M^{(p)}(s)$ stands for the derivative of order p; functions *gamma*, *incomplete gamma*, and *complementary incomplete gamma* are defined as

$\Gamma(\kappa) = (\kappa-1)!$, $\gamma(\kappa, x) = \int_0^x t^{\kappa-1}e^{-t}dt$, $\Gamma(\kappa, x) = \int_x^\infty t^{\kappa-1}e^{-t}dt$ [42, Eqns. (2.4), (2.39), (2.40)], respectively. Finally, $(N)_n$ is the Pochhammer symbol [42, p. 273], i.e., $(N)_0 = 1$ and $(N)_n = N(N+1)\dots(N+n-1), \forall n > 1$, and ${}_1F_1(\cdot;\cdot;\cdot)$ is a generalized hypergeometric function [43, Section 18.9.1] [44, Chapter 13] also known as the confluent hypergeometric function [42, Eq. (10.8), p. 323] [42, Eq. (9.1), p. 299].

D. Paper Organization

Section II introduces our statistical models for the transmitted signal, noise, and channel fading. Section III derives the exact m.g.f., p.d.f., and moments for the SNR of MIMO ZF in Rician–Rayleigh fading. Then, Section IV derives important performance measures for ZF, e.g., the diversity order, AEP, outage probability, and ergodic capacity. Section V presents numerical results from our analysis and Monte Carlo simulations. Appendix A sketches from [20, Section 3] the derivation of the ZF SNR for the intended stream conditioned on the channel matrix of the interferers. Finally, Appendix B discusses SIMO ($N_\mathrm{T} = 1$) maximal ratio combining (MRC) as a special case of MIMO ZF, and Rayleigh fading as a special case of Rician fading, revealing analogies and confirming that our analysis results reduce for these cases to previous results.

II. Signal, Noise, and Fading Models

We consider an uncoded multiantenna-based wireless communication system over a frequency-flat fading channel. As mentioned, we assume that there are N_T and N_R antenna elements at the transmitter and receiver, respectively, with $N_\mathrm{T} \le N_\mathrm{R}$. Letting $\mathbf{x} = [x_1\, x_2\, \cdots\, x_{N_\mathrm{T}}]^\mathcal{T}$ denote the $N_\mathrm{T} \times 1$ zero-mean transmit-symbol vector with $\mathbb{E}\{\mathbf{x}\mathbf{x}^\mathcal{H}\} = \mathbf{I}_{N_\mathrm{T}}$, the $N_\mathrm{R} \times 1$ vector with the received signals can be represented as [2, p. 63]:

$$\mathbf{r} = \sqrt{\frac{E_\mathrm{s}}{N_\mathrm{T}}}\,\mathbf{H}\mathbf{x} + \mathbf{n}. \tag{1}$$

Above, $E_\mathrm{s}/N_\mathrm{T}$ is the energy transmitted per symbol (i.e., per antenna), so that E_s is the energy transmitted per channel use. The additive noise vector $\mathbf{n}$ is uncorrelated, circularly-symmetric, zero-mean, complex Gaussian with $\mathbf{n} \sim \mathcal{N}_\mathrm{c}(\mathbf{0}, N_0\,\mathbf{I}_{N_\mathrm{R}})$ [45]. Finally, $\mathbf{H}$ is the $N_\mathrm{R} \times N_\mathrm{T}$ complex-Gaussian channel matrix, assumed to have rank N_T. The deterministic (i.e., mean) and random components of $\mathbf{H}$ are denoted as $\mathbf{H}_\mathrm{d}$ and $\mathbf{H}_\mathrm{r}$, respectively, so that $\mathbf{H} = \mathbf{H}_\mathrm{d} + \mathbf{H}_\mathrm{r}$. If $[\mathbf{H}_\mathrm{d}]_{i,j} = 0$ then $|\,[\mathbf{H}]_{i,j}\,|$ has a Rayleigh distribution; otherwise, $|\,[\mathbf{H}]_{i,j}\,|$ has a Rician distribution [3].

Typically, the channel matrix for Rician fading is written as [2, p. 41] [46] [47]

$$\mathbf{H} = \mathbf{H}_{\text{d}} + \mathbf{H}_{\text{r}} = \sqrt{\frac{K}{K+1}}\,\mathbf{H}_{\text{d,n}} + \sqrt{\frac{1}{K+1}}\,\mathbf{H}_{\text{r,n}}, \tag{2}$$

where it is assumed for normalization purposes that $\|\mathbf{H}_{\text{d,n}}\|^2 = N_{\text{T}}N_{\text{R}}$ and $\mathbb{E}\{|\,[\mathbf{H}_{\text{r,n}}]_{i,j}\,|^2\} = 1, \forall i, j$, so that $\mathbf{E}\{\|\mathbf{H}\|^2\} = N_{\text{T}}N_{\text{R}}$ [46] [47] [48]. Power ratio

$$\frac{\|\mathbf{H}_{\text{d}}\|^2}{\mathbb{E}\{\|\mathbf{H}_{\text{r}}\|^2\}} = \frac{\frac{K}{K+1}\|\mathbf{H}_{\text{d,n}}\|^2}{\frac{1}{K+1}\mathbb{E}\{\|\mathbf{H}_{\text{r,n}}\|^2\}} = K \tag{3}$$

is known as the Rician K-factor. Then, $K = 0$ yields Rayleigh fading, because $\mathbf{H}_{\text{d}} = \mathbf{0}$ and $\mathbf{H}_{\text{r}} = \mathbf{H}_{\text{r,n}}$. On the other hand, $K \neq 0$ can yield Rician fading. WINNER II [24] has modeled measured K (in dB) as a random variable with scenario-dependent lognormal distribution.

Throughout this paper, we assume zero receive-correlation. On the other hand, we assume nonzero transmit-correlation. We also need to assume, for tractability, as in previous work [19] [20], that all transposed rows of $\mathbf{H}_{\text{r,n}}$ have distribution $\mathcal{N}_{\text{c}}(\mathbf{0}, \mathbf{R}_{\text{T}})$. Then, all transposed rows of $\mathbf{H}_{\text{r}}$ have distribution $\mathcal{N}_{\text{c}}(\mathbf{0}, \mathbf{R}_{\text{T},K})$, where $\mathbf{R}_{\text{T},K} = \frac{1}{K+1}\mathbf{R}_{\text{T}}$.

Then, the elements of $\mathbf{R}_{\text{T}}$ can be computed from the AS as shown in [26, Section VI.A] when assuming Laplacian power azimuth spectrum, as in WINNER II. Note that, WINNER II [24] has modeled measured AS (in degrees) as a random variable with scenario-dependent lognormal distribution. Other measurement-based work expressed the power azimuth spectrum in more detail, i.e., in terms of the base station antenna, average building height, base–mobile distance, etc.— see [27] and references therein.

III. Exact SNR M.G.F. and P.D.F. Derivation for MIMO ZF

A. ZF Symbol-Detection SNR in Conventional (Ratio) and Hermitian Forms

Given $\mathbf{H}$ and nonsingular $\mathbf{W} = \mathbf{H}^{\mathcal{H}}\mathbf{H}$, ZF for the signal from (1) means separately mapping each element of the following vector into the closest modulation constellation symbol [2, p. 153] [49]:

$$\sqrt{\frac{N_{\text{T}}}{E_{\text{s}}}}\left[\mathbf{H}^{\mathcal{H}}\mathbf{H}\right]^{-1}\mathbf{H}^{\mathcal{H}}\,\mathbf{r} = \mathbf{x} + \sqrt{\frac{N_{\text{T}}}{E_{\text{s}}}}\left[\mathbf{H}^{\mathcal{H}}\mathbf{H}\right]^{-1}\mathbf{H}^{\mathcal{H}}\mathbf{n}. \tag{4}$$

There is no interference among the transmitted streams, which explains the ZF name for this technique. However, the noise vector that corrupts the transmitted signal vector $\mathbf{x}$ in (4) has correlation matrix $\frac{N_{\text{T}}N_0}{E_{\text{s}}}\mathbf{W}^{-1}$. Thus, ZF is suboptimal because, although the noise vector elements are mutually correlated, the streams are detected independently. Furthermore, ZF yields noise enhancement when $\mathbf{W}$ is poorly-conditioned. Nevertheless, ZF has low complexity, e.g., compared to the maximum-likelihood approach, for large N_{T} and modulation constellations [2, p. 153] [49]. Also, unlike MMSE, ZF does not require knowledge of the noise variance.

From (4), the SNR for stream $k = 1$ is readily expressed in the ratio form

$$\gamma_1 = \frac{\frac{E_{\mathrm{s}}}{N_0}\frac{1}{N_{\mathrm{T}}}}{\left[\mathbf{W}^{-1}\right]_{1,1}}, \tag{5}$$

that has been employed typically in ZF studies [19] [21] [26] [28]. Then, by partitioning $N_{\mathrm{T}} \times N_{\mathrm{T}}$ matrix $\mathbf{W}$, scalar γ_1 can be written as the determinant of the Schur complement of a submatrix of $\mathbf{W}$ [19, Eq. 8]. When all the elements of channel matrix $\mathbf{H}$ are Rayleigh-fading, $\mathbf{W}$ has a central-Wishart distribution with N_{R} degrees of freedom [50, p. 82]. Then, the Schur-complement determinant that enters γ_1 is a scalar that has a central-Wishart distribution with $N = N_{\mathrm{R}} - N_{\mathrm{T}} + 1$ degrees of freedom [19, Theorem], i.e., γ_1 is Gamma-distributed [19] for the special case of Rayleigh fading. On the other hand, when some of the channel-matrix elements are Rician-fading, matrix $\mathbf{W}$ has a noncentral-Wishart distribution and the distribution of γ_1 is unknown. Therefore, [26] evaluated an approximation of the noncentral-Wishart distribution with a central-Wishart distribution of equal mean. However, as explained in [26] and later in Section V, this approximation is not always reliable.

The Wishart distribution can be bypassed by rewriting the ZF SNR as a Hermitian form, as shown next from [20]. Instead of partitioning $\mathbf{W} = \mathbf{H}^{\mathcal{H}}\mathbf{H}$ as done in [19], let us partition the channel matrix $\mathbf{H}$ itself as

$$\mathbf{H} = \left[\mathbf{h}_1 \mid \widetilde{\mathbf{H}}\right] = \left[\mathbf{h}_{1,\mathrm{d}} \mid \widetilde{\mathbf{H}}_{\mathrm{d}}\right] + \left[\mathbf{h}_{1,\mathrm{r}} \mid \widetilde{\mathbf{H}}_{\mathrm{r}}\right], \tag{6}$$

where $\mathbf{h}_1$ is the $N_{\mathrm{R}} \times 1$ channel vector corresponding to the intended stream, and $\widetilde{\mathbf{H}}$ is the $N_{\mathrm{R}} \times (N_{\mathrm{T}} - 1)$ matrix, assumed of rank $N_{\mathrm{T}} - 1$, with the channel vectors corresponding to the interfering streams. Then, as in [20], we can rewrite γ_1 from (5) as

$$\gamma_1 = \frac{E_{\mathrm{s}}}{N_0}\frac{1}{N_{\mathrm{T}}}\mathbf{h}_1^{\mathcal{H}} \underbrace{\left[\mathbf{I}_{N_{\mathrm{R}}} - \widetilde{\mathbf{H}}\left(\widetilde{\mathbf{H}}^{\mathcal{H}}\widetilde{\mathbf{H}}\right)^{-1}\widetilde{\mathbf{H}}^{\mathcal{H}}\right]}_{=\mathbf{Q}}\mathbf{h}_1 = \frac{E_{\mathrm{s}}}{N_0}\frac{1}{N_{\mathrm{T}}}\mathbf{h}_1^{\mathcal{H}}\mathbf{Q}\mathbf{h}_1, \tag{7}$$

where the $N_{\mathrm{R}} \times N_{\mathrm{R}}$ Hermitian matrices $\widetilde{\mathbf{H}}\left(\widetilde{\mathbf{H}}^{\mathcal{H}}\widetilde{\mathbf{H}}\right)^{-1}\widetilde{\mathbf{H}}^{\mathcal{H}}$ and $\mathbf{Q}$ are idempotent, have ranks

$N_\mathrm{T}-1$ and N, respectively, and have eigenvalues as listed below:

$$\widetilde{\mathbf{H}}\left(\widetilde{\mathbf{H}}^{\mathcal{H}}\widetilde{\mathbf{H}}\right)^{-1}\widetilde{\mathbf{H}}^{\mathcal{H}}: \; 1,\ 1,\ \ldots,\ 1,\ \ 0,\ 0,\ \ldots,\ 0. \tag{8}$$

$$\mathbf{Q}: \; \underbrace{0,\ 0,\ \ldots,\ 0,}_{N_\mathrm{T}-1}\ \ \underbrace{1,\ 1,\ \ldots,\ 1}_{N}. \tag{9}$$

Next, the m.g.f. of the SNR from (7) is derived by first conditioning on $\widetilde{\mathbf{H}}$ (i.e., $\mathbf{Q}$) and then by averaging over it.

B. Derivation of the M.G.F. of the Conditioned SNR

Since $\mathbf{h}_1$ and the columns of $\widetilde{\mathbf{H}}$ are assumed correlated in (6), conditioning γ_1 on $\widetilde{\mathbf{H}}$ based on (7) requires explicit conditioning of $\mathbf{h}_1$ on $\widetilde{\mathbf{H}}$ (i.e., $\mathbf{Q}$). For this, we follow the procedure from [20, Section 3] in Appendix A, to recast the distribution of γ_1 conditioned on $\mathbf{Q}$ as

$$\gamma_1|\mathbf{Q} \;=\; \Gamma_1 \mathbf{x}_1^{\mathcal{H}}\mathbf{Q}\mathbf{x}_1, \tag{10}$$

$$\Gamma_1 \;=\; \frac{E_\mathrm{s}}{N_0}\frac{1}{N_\mathrm{T}}\frac{1}{\left[\mathbf{R}_{\mathrm{T},K}^{-1}\right]_{1,1}}, \tag{11}$$

$$\mathbf{x}_1 \;\sim\; \mathcal{N}_\mathrm{c}\left(\sqrt{\left[\mathbf{R}_{\mathrm{T},K}^{-1}\right]_{1,1}}\,\boldsymbol{\mu}, \mathbf{I}_{N_\mathrm{R}}\right), \tag{12}$$

with $\boldsymbol{\mu}$ deterministic and defined in (44) in Appendix A.

Using Turin's result from [51, Eq. (4a)], the m.g.f. of γ_1 given $\mathbf{Q}$ can be written as

$$\begin{aligned} M_{\gamma_1|\mathbf{Q}}(s) &= \mathbb{E}_{\gamma_1|\mathbf{Q}}\{e^{s\gamma_1}|\mathbf{Q}\} \\ &= |\mathbf{I}_{N_\mathrm{R}} - s\Gamma_1\mathbf{Q}|^{-1}\exp\{-\left[\mathbf{R}_{\mathrm{T},K}^{-1}\right]_{1,1}\boldsymbol{\mu}^{\mathcal{H}}\left[\mathbf{I}_{N_\mathrm{R}} - (\mathbf{I}_{N_\mathrm{R}} - s\Gamma_1\mathbf{Q})^{-1}\right]\boldsymbol{\mu}\}. \end{aligned} \tag{13}$$

The natural next step is to average $M_{\gamma_1|\mathbf{Q}}(s)$ from (13) over $\mathbf{Q}$, which is performed in the next subsection, but this requires the following further manipulation of $M_{\gamma_1|\mathbf{Q}}(s)$. First, let us consider the singular value decomposition $\widetilde{\mathbf{H}} = \mathbf{U}\boldsymbol{\Sigma}\mathbf{V}^{\mathcal{H}}$, where $N_\mathrm{R}\times N_\mathrm{R}$ matrix $\mathbf{U}$ and $(N_\mathrm{T}-1)\times(N_\mathrm{T}-1)$ matrix $\mathbf{V}$ are unitary, i.e., $\mathbf{U}^{\mathcal{H}}\mathbf{U} = \mathbf{U}\mathbf{U}^{\mathcal{H}} = \mathbf{I}_{N_\mathrm{R}}$ and $\mathbf{V}^{\mathcal{H}}\mathbf{V} = \mathbf{V}\mathbf{V}^{\mathcal{H}} = \mathbf{I}_{N_\mathrm{T}-1}$, and $N_\mathrm{R}\times(N_\mathrm{T}-1)$ matrix $\boldsymbol{\Sigma}$ is the matrix with the singular values of $\widetilde{\mathbf{H}}$. Then, it can be shown that $\mathbf{Q} = \mathbf{I}_{N_\mathrm{R}} - \widetilde{\mathbf{H}}\left(\widetilde{\mathbf{H}}^{\mathcal{H}}\widetilde{\mathbf{H}}\right)^{-1}\widetilde{\mathbf{H}}^{\mathcal{H}}$ has the eigendecomposition $\mathbf{Q} = \mathbf{U}^{\mathcal{H}}\boldsymbol{\Lambda}_N\mathbf{U}$. We assume that diagonal matrix $\boldsymbol{\Lambda}_N$ has the N unit-valued eigenvalues of $\mathbf{Q}$ grouped at the top-left on its main diagonal. Since only $\mathbf{U}$ is random, the conditioning of γ_1 on $\mathbf{Q}$ from (13) reduces to the conditioning of γ_1 on

$\mathbf{U}$. By defining the $N_{\mathrm{R}} \times 1$ deterministic unit-norm vector $\boldsymbol{\mu}_1 = \boldsymbol{\mu}/\|\boldsymbol{\mu}\|$, further manipulating (13) yields

$$M_{\gamma_1|\mathbf{U}}(s) = \frac{1}{(1-\Gamma_1 s)^N} \exp\Big\{ \underbrace{\left[\mathbf{R}_{\mathrm{T},K}^{-1}\right]_{1,1} \|\boldsymbol{\mu}\|^2}_{=\alpha} \frac{\Gamma_1 s}{1-\Gamma_1 s} \boldsymbol{\mu}_1^{\mathcal{H}} \mathbf{U} \boldsymbol{\Lambda}_N \underbrace{\mathbf{U}^{\mathcal{H}} \boldsymbol{\mu}_1}_{=\boldsymbol{\nu}_1} \Big\}, \tag{14}$$

$$= \frac{1}{(1-\Gamma_1 s)^N} \exp\left\{\alpha \frac{\Gamma_1 s}{1-\Gamma_1 s} \boldsymbol{\nu}_1^{\mathcal{H}} \boldsymbol{\Lambda}_N \boldsymbol{\nu}_1\right\} = M_{\gamma_1|\boldsymbol{\nu}_1}(s), \tag{15}$$

where $\boldsymbol{\nu}_1$ is a random $N_{\mathrm{R}} \times 1$ vector whose distribution is discussed below.

C. Special Case: Rician–Rayleigh Fading

The analysis presented heretofore holds for the general case when any element of the channel matrix may experience Rician fading. On the other hand, the analysis presented hereafter applies only for the special case of Rician–Rayleigh fading, whereby stream 1 may experience Rician fading whereas streams $i = 2 : N_{\mathrm{T}}$ experience Rayleigh fading, i.e., $\widetilde{\mathbf{H}}_{\mathrm{d}} = \mathbf{0}_{N_{\mathrm{R}} \times (N_{\mathrm{T}}-1)}$ in (6). Although this assumption reduces the generality of our results it is required for tractability[4].

Since matrix $\widetilde{\mathbf{H}}$ is zero-mean complex-valued Gaussian distributed, matrix $\mathbf{U}$ is isotropically (also known as Haar) distributed on the group of $N_{\mathrm{R}} \times N_{\mathrm{R}}$ unitary matrices[5] [52, Lemma 1] [1, Appendix A.2] [53, §3] [17, Appendix A]. Because $\mathbf{U}$ is isotropically distributed and $\boldsymbol{\mu}_1$ is deterministic and belongs to the subset $\Omega_{N_{\mathrm{R}}}$ of unit-norm vectors, $\boldsymbol{\nu}_1$ is isotropically distributed on $\Omega_{N_{\mathrm{R}}}$ [52, Lemma 2] [1, Appendix A.2]. Now, it is also known, from [1, Appendix A.1], that if $\mathbf{z} \sim \mathcal{N}_{\mathrm{c}}(\mathbf{0}, \mathbf{I}_{N_{\mathrm{R}}})$, then $\frac{\mathbf{z}}{\|\mathbf{z}\|}$ is isotropically distributed on the subset $\Omega_{N_{\mathrm{R}}}$. Thus, $\boldsymbol{\nu}_1 \simeq \frac{\mathbf{z}}{\|\mathbf{z}\|}$, and so

$$\boldsymbol{\nu}_1^{\mathcal{H}} \boldsymbol{\Lambda}_N \boldsymbol{\nu}_1 \simeq \frac{\mathbf{z}^{\mathcal{H}}}{\|\mathbf{z}\|} \boldsymbol{\Lambda}_N \frac{\mathbf{z}}{\|\mathbf{z}\|} = \frac{\mathbf{z}^{\mathcal{H}} \boldsymbol{\Lambda}_N \mathbf{z}}{\|\mathbf{z}\|^2} = \frac{\mathbf{z}^{\mathcal{H}} \boldsymbol{\Lambda}_N \mathbf{z}}{\mathbf{z}^{\mathcal{H}} \mathbf{I}_{N_{\mathrm{R}}} \mathbf{z}} \triangleq \eta_1, \tag{16}$$

i.e., η_1 is a new random variable of the same distribution as $\boldsymbol{\nu}_1^{\mathcal{H}} \boldsymbol{\Lambda}_N \boldsymbol{\nu}_1$. Substituting η_1 in (15) yields

$$M_{\gamma_1|\boldsymbol{\nu}_1}(s) \simeq M_{\gamma_1|\eta_1}(s) = \frac{1}{(1-\Gamma_1 s)^N} \exp\left\{\alpha \frac{\Gamma_1 s}{1-\Gamma_1 s} \eta_1\right\}. \tag{17}$$

[4]It is also required for the Bartlett decomposition of a noncentral-Wishart distributed matrix in [50, Theorem 10.3.8, p. 448].

[5]Therefore, the $N_{\mathrm{R}} \times N$ submatrix $\mathbf{U}_N$ of $\mathbf{U}$ comprising its first N columns has uniform distribution over the Stiefel $(N_{\mathrm{R}}, N_{\mathrm{T}})$ manifold [17, Appendix A].

D. Averaging the M.G.F. of the Conditioned SNR

Averaging (17) over η_1 yields

$$M_{\gamma_1}(s) \;=\; \mathbb{E}_{\eta_1}\{M_{\gamma_1|\eta_1}(s)\} = \frac{1}{(1-\Gamma_1 s)^N} M_{\eta_1}\left(\alpha \frac{\Gamma_1 s}{1-\Gamma_1 s}\right), \tag{18}$$

where $M_{\eta_1}(t)$ is the m.g.f. of η_1, which is derived next. Let us rewrite η_1 from (16) as follows:

$$\eta_1 = \frac{\sum_{i=1}^{N} |z_i|^2}{\sum_{i=1}^{N_\mathrm{R}} |z_i|^2} = \frac{\sum_{i=1}^{N} |z_i|^2}{\sum_{i=1}^{N} |z_i|^2 + \sum_{i=N+1}^{N_\mathrm{R}} |z_i|^2} = \frac{\frac{2N}{2(N_\mathrm{R}-N)} \left[\frac{\sum_{i=1}^{N} |z_i|^2}{2N}\right] / \left[\frac{\sum_{i=N+1}^{N_\mathrm{R}} |z_i|^2}{2(N_\mathrm{R}-N)}\right]}{\frac{2N}{2(N_\mathrm{R}-N)} \left[\frac{\sum_{i=1}^{N} |z_i|^2}{2N}\right] / \left[\frac{\sum_{i=N+1}^{N_\mathrm{R}} |z_i|^2}{2(N_\mathrm{R}-N)}\right] + 1}. \tag{19}$$

Note that $\sum_{i=1}^{N} |z_i|^2 \sim \chi^2(2N)$ and $\sum_{i=N+1}^{N_\mathrm{R}} |z_i|^2 \sim \chi^2(2(N_\mathrm{R}-N))$ [54, Ch. 18]. Because they are also independent, we have that [43, Section 6.4.3, §2]

$$\left[\frac{\sum_{i=1}^{N} |z_i|^2}{2N}\right] / \left[\frac{\sum_{i=N+1}^{N_\mathrm{R}} |z_i|^2}{2(N_\mathrm{R}-N)}\right] \sim F(2N, 2(N_\mathrm{R}-N)), \tag{20}$$

i.e., the Fisher–Snedecor distribution with parameters $2N$ and $2(N_\mathrm{R}-N)$ [54, Ch. 27] [43, Section 6.8]. Therefore, the distribution of η_1 from (19) is [54, Vol. 2, p. 327] [43, Section 6.8.3, §4] [44, §26.5.3, p. 944]

$$\eta_1 = \frac{\mathbf{z}^{\mathcal{H}} \mathbf{\Lambda}_N \mathbf{z}}{\mathbf{z}^{\mathcal{H}} \mathbf{I}_{N_\mathrm{R}} \mathbf{z}} \sim Beta(N, N_\mathrm{R}-N), \tag{21}$$

i.e., η_1 is Beta distributed with shape parameters N and $N_\mathrm{R}-N$ [54, Ch. 25]. Therefore, the m.g.f. of η_1 is [43, Section 6.2.1]

$$M_{\eta_1}(\sigma) = \sum_{n=0}^{\infty} \underbrace{\frac{(N)_n}{(N_\mathrm{R})_n} \frac{\sigma^n}{n!}}_{=A_n(\sigma)} = {}_1F_1(N; N_\mathrm{R}; \sigma), \quad \forall \sigma \in \mathbb{R}, \tag{22}$$

whereby the infinite sum converges for any σ [42, p. 332] [42, Eq. (9.1), p. 299]. Finally, replacing (22) into (18) yields the following m.g.f. for the ZF SNR in Rician–Rayleigh fading:

$$M_{\gamma_1}(s) = \frac{1}{(1-\Gamma_1 s)^N} \, {}_1F_1\left(N; N_\mathrm{R}; \alpha \frac{\Gamma_1 s}{1-\Gamma_1 s}\right). \tag{23}$$

Our earlier assumption that the interfering streams experience Rayleigh fading, i.e., $\widetilde{\mathbf{H}}_\mathrm{d} = \mathbf{0}_{N_\mathrm{R} \times (N_\mathrm{T}-1)}$, and (44) in Appendix A, yield $\boldsymbol{\mu} = \mathbf{h}_{1,\mathrm{d}}$. Thus, $\|\boldsymbol{\mu}\|^2 = \|\mathbf{h}_{1,\mathrm{d}}\|^2 = \|\left[\mathbf{h}_{1,\mathrm{d}} \mid \mathbf{0}_{N_\mathrm{R} \times (N_\mathrm{T}-1)}\right]\|^2 = \|\mathbf{H}_\mathrm{d}\|^2 = \frac{K}{K+1} N_\mathrm{R} N_\mathrm{T}$, and, from (14), $\alpha = K N_\mathrm{R} N_\mathrm{T} \left[\mathbf{R}_\mathrm{T}^{-1}\right]_{1,1}$. Interestingly, ZF performance in Rician fading is affected by transmit correlation only through scalar $\left[\mathbf{R}_\mathrm{T}^{-1}\right]_{1,1}$, and by $\mathbf{h}_{1,\mathrm{d}}$ only through $\|\mathbf{h}_{1,\mathrm{d}}\|$. The particular magnitudes and phases of the elements of $\mathbf{h}_{1,\mathrm{d}}$, i.e., its 'direction', do not affect performance. This directional information gets discarded because $\mathbf{U}^{\mathcal{H}}\boldsymbol{\mu}_1$ in (14) has the same (isotropic) distribution for any $\boldsymbol{\mu}_1$.

Appendix B shows that the MIMO ZF SNR m.g.f. expression derived above for Rician fading reduces to that derived in previous work for SIMO ($N_{\mathrm{T}} = 1$) MRC. It also reveals that a performance analogy is possible between MIMO ZF and SIMO MRC for Rayleigh fading but not for Rician fading. Finally, it discusses per-stream performance-measure expression availability for MIMO ZF in Rician–Rayleigh and Rayleigh-Rayleigh fading.

E. Infinite Linear Combination of Gamma Distributions for ZF SNR

Based on (22), we can write the hypergeometric-function term from (23) as

$$
\begin{aligned}
{}_1F_1\left(N; N_{\mathrm{R}}; \alpha\frac{\Gamma_1 s}{1-\Gamma_1 s}\right) &= \sum_{n=0}^{\infty}\frac{(N)_n}{(N_{\mathrm{R}})_n}\frac{1}{n!}\left(\alpha\frac{s\Gamma_1}{1-s\Gamma_1}\right)^n = \sum_{n=0}^{\infty}\underbrace{\frac{(N)_n}{(N_{\mathrm{R}})_n}\frac{\alpha^n}{n!}}_{=A_n(\alpha)}\left(\frac{s\Gamma_1}{1-s\Gamma_1}\right)^n \\
&= \sum_{n=0}^{\infty}A_n(\alpha)\left(-1+\frac{1}{1-s\Gamma_1}\right)^n = \sum_{n=0}^{\infty}A_n(\alpha)\sum_{m=0}^{n}\binom{n}{m}(-1)^m\left(\frac{1}{1-s\Gamma_1}\right)^{n-m},
\end{aligned}
$$

so that the ZF SNR m.g.f. from (23) can be recast as

$$
M_{\gamma_1}(s) = \sum_{n=0}^{\infty}A_n(\alpha)\sum_{m=0}^{n}\binom{n}{m}(-1)^m\underbrace{\frac{1}{(1-s\Gamma_1)^{N+n-m}}}_{=M_{n,m}(s)}. \tag{24}
$$

Notice that $M_{n,m}(s)$ is the m.g.f. of a Gamma distribution with *shape* parameter $N+n-m$ and *scale* parameter Γ_1, whose p.d.f. is then [26, Section IV.D] [43, Section 6.9.1]:

$$
p_{m,n}(t) = \frac{t^{(N+n-m)-1}e^{-t/\Gamma_1}}{[(N+n-m)-1]!\,\Gamma_1^{N+n-m}}, \quad t \geq 0. \tag{25}
$$

Thus, the ZF SNR p.d.f. corresponding to the m.g.f. from (24) is expressed as the following infinite linear combination of p.d.f.s of Gamma distributions:

$$
p_{\gamma_1}(t) = \sum_{n=0}^{\infty}A_n(\alpha)\sum_{m=0}^{n}\binom{n}{m}(-1)^m p_{m,n}(t), \quad t \geq 0. \tag{26}
$$

For Rayleigh fading, i.e., $\alpha = 0$, only the terms for $n = m = 0$ remain from (24) and (26), which yield the following, known, expressions for the ZF SNR m.g.f. and p.d.f. [19] [20]:

$$
M_{\gamma_1,\mathrm{Rayleigh}}(s) = \frac{1}{(1-s\Gamma_1)^N} \tag{27}
$$

$$
p_{\gamma_1,\mathrm{Rayleigh}}(t) = \frac{t^{N-1}e^{-t/\Gamma_1}}{(N-1)!\,\Gamma_1^N}, \quad t \geq 0, \tag{28}
$$

i.e., the ZF SNR has a Gamma distribution with shape parameter N and scale parameter Γ_1.

TABLE I

MOMENTS, VARIANCE, AND AMOUNT OF FADING FOR γ_1

	Rician	Rayleigh
$\mathbb{E}\{\gamma_1\} = M^{(1)}(0)$	$N\,\Gamma_1\left(1+\frac{\alpha}{N_\mathrm{R}}\right)$	$N\,\Gamma_1$
$\mathbb{E}\{\gamma_1^2\} = M^{(2)}(0)$	$N(N+1)\,\Gamma_1^2\left[\left(1+\frac{\alpha}{N_\mathrm{R}}\right)^2-\frac{\alpha^2}{N_\mathrm{R}^2}\frac{1}{(N_\mathrm{R}+1)}\right]$	$N(N+1)\,\Gamma_1^2$
$\mathbb{V}\{\gamma_1\} = \mathbb{E}\{\gamma_1^2\}-(\mathbb{E}\{\gamma_1\})^2$	$N\Gamma_1^2\left[\left(1+\frac{\alpha}{N_\mathrm{R}}\right)^2-\frac{\alpha^2}{N_\mathrm{R}^2}\frac{N+1}{(N_\mathrm{R}+1)}\right]$	$N\Gamma_1^2$
$\mathbb{A}\{\gamma_1\} = \mathbb{V}\{\gamma_1\}/(\mathbb{E}\{\gamma_1\})^2$	$\frac{1}{N}\left[1-\frac{N+1}{N_\mathrm{R}+1}\frac{\alpha^2}{(\alpha+N_\mathrm{R})^2}\right]$	$\frac{1}{N}$

F. Moments of MIMO ZF SNR

By using in (23) the following ${}_1F_1(\cdot;\cdot;\cdot)$ derivative property [42, p. 300]

$$\frac{d^p}{d\sigma^p}\,{}_1F_1\left(N;N_\mathrm{R};\sigma\right) = \frac{(N)_p}{(N_\mathrm{R})_p}\,{}_1F_1\left(N+p;N_\mathrm{R}+p;\sigma\right), \tag{29}$$

we have obtained, with some difficulty, closed-form expressions for the first two derivatives of $M_{\gamma_1}(s)$, which are not shown. From them, we have expressed in Table I the corresponding SNR moments as well as the SNR variance $\mathbb{V}\{\gamma_1\}$ and the amount of fading $\mathbb{A}\{\gamma_1\}$ [3, p. 18], for Rician and Rayleigh fading. The top line reveals that Rician fading improves the average SNR by a factor of $1+\frac{\alpha}{N_\mathrm{R}} = 1+KN_\mathrm{T}\left[\mathbf{R}_\mathrm{T}^{-1}\right]_{1,1}$ vs. Rayleigh fading.

Using (23) and (29) to derive closed-form expressions for SNR moments of order $p=3,4,\ldots$ becomes increasingly tedious. On the other hand, from our alternative SNR m.g.f. expression in (24) we can easily express the derivative of any order p of $M_{\gamma_1}(s)$ as the infinite sum

$$M_{\gamma_1}^{(p)}(s) = \Gamma_1^p\sum_{n=0}^{\infty}A_n(\alpha)\sum_{m=0}^{n}\binom{n}{m}(-1)^m\frac{(N+n-m)_p}{(1-s\Gamma_1)^{N+n-m+p}}, \tag{30}$$

which yields the moment of order p of γ_1 as follows

$$\mathbb{E}\{\gamma_1^p\} = M_{\gamma_1}^{(p)}(0) = \Gamma_1^p\sum_{n=0}^{\infty}A_n(\alpha)\sum_{m=0}^{n}\binom{n}{m}(-1)^m(N+n-m)_p. \tag{31}$$

IV. ZF Performance Measures

A. ZF Diversity Order

The diversity order is the AEP slope magnitude when the transmit-SNR, i.e., $\frac{E_\mathrm{s}}{N_0}$, grows large. Now, the MIMO ZF SNR m.g.f. expression from (24) can be rewritten as

$$\begin{aligned} M_{\gamma_1}(s) &= \frac{1}{s^N} + \sum_{n=1}^{\infty} A_n(\alpha) \sum_{m=0}^{n} \binom{n}{m} (-1)^m \frac{1}{(1 - s\Gamma_1)^{N+n-m}} \\ &= \frac{1}{s^N} + \mathcal{O}\left(\frac{1}{s^{N+1}}\right). \end{aligned} \tag{32}$$

According to [55, Proposition 1], a transmit–receive scheme whose SNR m.g.f. can be expressed as in (32) has diversity order N. Thus, ZF has diversity order N for both Rician and Rayleigh fading[6]. Nevertheless, there is an array gain[7] with Rician fading over Rayleigh fading, as shown in Section V.

B. Exact ZF AEP and Outage Probability Expressions

When the SNR m.g.f. expression is available, one can apply the elegant AEP-derivation procedure from [3, Chapter 9], e.g., for MPSK modulation (the same procedure also applies for other modulations). Given γ_1, the error probability for stream 1 can be written as [3, Eq. (8.22)]

$$P_\mathrm{e}(\gamma_1) = \frac{1}{\pi} \int_0^{\frac{M-1}{M}\pi} \exp\left\{ -\gamma_1 \frac{\sin^2 \frac{\pi}{M}}{\sin^2 \theta} \right\} d\theta. \tag{33}$$

Then, the AEP can be written in terms of the m.g.f. of γ_1 as follows [3, Chapter 9]:

$$P_{\mathrm{e},1} = \mathbb{E}\{P_\mathrm{e}(\gamma_1)\} = \frac{1}{\pi} \int_0^{\frac{M-1}{M}\pi} M_{\gamma_1}\left(-\frac{\sin^2 \frac{\pi}{M}}{\sin^2 \theta} \right) d\theta. \tag{34}$$

Substituting (23) into (34) yields the following exact ZF AEP expression for the stream that experiences Rician fading when all the other streams experience Rayleigh fading:

$$P_{\mathrm{e},1} = \frac{1}{\pi} \int_0^{\frac{M-1}{M}\pi} \left(\frac{\sin^2\theta}{\sin^2\theta + \Gamma_1 \sin^2 \frac{\pi}{M}} \right)^N {}_1F_1\left(N; N_\mathrm{R}; -\alpha \frac{\Gamma_1 \sin^2 \frac{\pi}{M}}{\sin^2\theta + \Gamma_1 \sin^2 \frac{\pi}{M}} \right) d\theta. \tag{35}$$

On the other hand, substituting (24) into (34) yields the equivalent exact ZF AEP expression

$$P_{\mathrm{e},1} = \textstyle\sum_{n=0}^{\infty} A_n(\alpha) \sum_{m=0}^{n} \binom{n}{m} (-1)^m \quad \displaystyle\frac{1}{\pi} \int_0^{\frac{M-1}{M}\pi} \left(\frac{\sin^2\theta}{\sin^2\theta + \Gamma_1 \sin^2 \frac{\pi}{M}} \right)^{N+n-m} d\theta. \tag{36}$$

[6]Because ZF employs $N_\mathrm{T} - 1$ degrees of freedom to cancel interference and the remaining N to yield diversity gain.

[7]Array gain is the left-shift of the plot AEP vs. $\frac{E_\mathrm{s}}{N_0}$, at large $\frac{E_\mathrm{s}}{N_0}$.

For Rayleigh fading, i.e., $\alpha = 0$, only the term for $n = m = 0$ remains from (36), i.e.,

$$P_{\text{e},1,\text{Rayleigh}} \quad = \quad \frac{1}{\pi} \int_0^{\frac{M-1}{M}\pi} \left(\frac{\sin^2\theta}{\sin^2\theta + \Gamma_1 \sin^2\frac{\pi}{M}} \right)^N d\theta. \tag{37}$$

Note that the integrals in (36) and (37) can be written in closed-form as explained in [56, Appendinx A].

Note that a ZF analysis approach based on the Wishart distribution approximation is described in [26]. There, the ZF SNR for fading that is allowed to be Rician–Rician is approximated as Gamma-distributed. Then, the same AEP derivation procedure as shown above yields the approximate AEP expression [26, Eq. (39)]. Its accuracy is compared to that of the exact AEP expression from (35) in Section V.

Finally, integrating (26), the ZF outage probability for the threshold SNR $\gamma_{1,\text{th}}$ is [3, Eq. (1.4)]

$$P_{\text{o}} = Pr(\gamma_1 \leq \gamma_{1,\text{th}}) = \sum_{n=0}^{\infty} A_n(\alpha) \sum_{m=0}^{n} \binom{n}{m} (-1)^m \frac{\gamma\left(N+n-m, \gamma_{1,\text{th}}/\Gamma_1\right)}{\Gamma(N+n-m)}. \tag{38}$$

Note that the outage probability is actually the SNR c.d.f.

C. *Exact ZF Ergodic Capacity Expression*

Given the SNR γ_1 at the ZF receiver, with p.d.f. expressed in (26), the instantaneous capacity in bits per channel use is $C(\gamma_1) = \log_2(1+\gamma_1)$ [57, Eq. (30)], and the ergodic capacity is defined as $\mathbb{E}_{\gamma_1}\{C(\gamma_1)\}$. Since the ergodic capacity corresponding to a virtual SNR with the Gamma p.d.f. from (25) is given by [57, Eq. (40)]

$$\overline{C}_{n,m}(N, \Gamma_1) = (\log_2 e) e^{1/\Gamma_1} \sum_{\kappa=0}^{N+n-m-1} \frac{\Gamma\left(-\kappa, 1/\Gamma_1\right)}{\Gamma_1^{\kappa}}, \tag{39}$$

the ZF ergodic capacity for Rician–Rayleigh fading can be expressed from (26) as follows:

$$\mathbb{E}_{\gamma_1}\{C(\gamma_1)\} = \sum_{n=0}^{\infty} A_n(\alpha) \sum_{m=0}^{n} \binom{n}{m} (-1)^m \overline{C}_{n,m}(N, \Gamma_1). \tag{40}$$

V. Numerical Results

Numerical results are presented for Rician–Rayleigh and Rayleigh–Rayleigh fading, $N_{\text{R}} = 4$, $N_{\text{T}} = 1 : 4$, stream $k = 1$, and relevant ranges of the average SNR per transmitted bit $\gamma_{\text{b}} = \frac{E_{\text{s}}}{N_0 N_{\text{T}}} \frac{1}{\log_2 M}$. Correlation matrix $\mathbf{R}_{\text{T}}$ has been computed as in [26], for a uniform linear antenna array with interelement distance normalized to carrier half wavelength $d_{\text{n}} = 1$, realistic Laplacian power azimuth spectrum centered at $\theta_{\mathrm{c}} = 5^{\circ}$, and values of K and AS, shown in dB and degrees, respectively, that are relevant from the perspective of the WINNER II model [26, Table I]. The shown AEP results are mostly from the new expression (35) and Monte Carlo simulations, but we also illustrate the Wishart-approximation-based AEP expression from [26, Eq. (39)].

Fig. 1 shows, for $N_{\mathrm{T}} = 4$, close agreement between the AEP from the new expression (35) and from simulation, which is consistent with our claim that (35) is exact. Fig. 1 also confirms a diversity order of $N = 1$ for both Rayleigh and Rician fading. Finally, Fig. 1 reveals a gap between the AEP from the approximate expression [26, Eq. (39)] and from simulation, although the Rician–Rayleigh scenario yields $\mathbf{H}_{\mathrm{d}}$ with $r = 1$, and [26] found the approximation generally accurate for rank-one $\mathbf{H}_{\mathrm{d}}$ generated as the outer product of receive and transmit array steering vectors. Other results (not shown) have revealed that the accuracy of the approximate AEP expression [26, Eq. (39)] degrades with increasing $N_{\mathrm{R}} - N_{\mathrm{T}}$ and with decreasing $N_{\mathrm{R}} = N_{\mathrm{T}}$. Also, other numerical results from our analysis and from simulations have confirmed that ZF performance is independent of the particular combination of magnitudes and phases of the elements of $\mathbf{h}_{1,\mathrm{d}}$.

Fig. 2 shows the AEP from the new expression (35) for SNR sufficiently high to reveal the ZF diversity order for all N_{T} choices (although the upper end of this SNR range yields some impractically-low AEP values). These results confirm that the diversity order is $N = N_{\mathrm{R}} - N_{\mathrm{T}} + 1$ for both Rician and Rayleigh fading, and that Rician fading outperforms Rayleigh fading by an array gain (dependent on N_{T}). As shown in [26], for outer-product-based $\mathbf{H}_{\mathrm{d}}$ (i.e., $r = 1$ and all streams experience Rician fading when $K \neq 0$), the AEP averaged over all streams reveals a diversity order of N, but Rician fading is outperformed by Rayleigh fading (i.e., K = 0).

Fig. 3 shows the AEP from exact expression (35), for QPSK modulation, $N_{\mathrm{T}} = 2$, $N_{\mathrm{R}} = 4$, and AS and K set to the averages for WINNER II scenarios A1 (indoor), C2 (typical urban macrocell), and D1 (rural macrocell) [26, Table I]. Note that $K = 7$ dB in all scenarios, for Rician–Rayleigh fading. For Rayleigh–Rayleigh fading, AEP decreases with increasing transmit AS, because of decreasing correlation. This performance improvement is due to array gain, since, as the figure also reveals, the diversity order is $N = N_{\mathrm{R}} - N_{\mathrm{T}} + 1 = 3$ for any AS. On the other hand, for Rician–Rayleigh fading, the AEP appears unaffected by transmit correlation. Simulation results (not shown, to avoid cluttering the figure) have confirmed this finding. For outer-product or all-ones $\mathbf{H}_{\mathrm{d}}$ (i.e., $r = 1$), earlier work found that the transmit AS affects the AEP

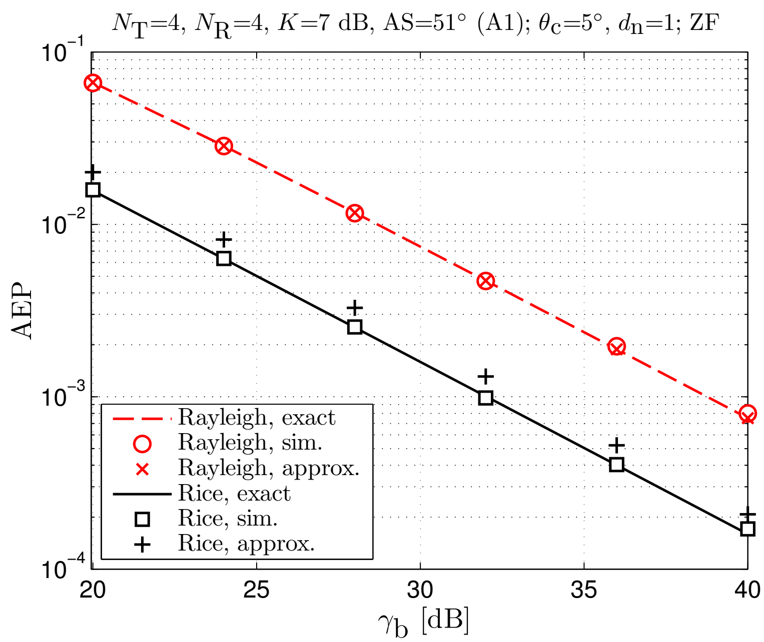

Fig. 1. AEP from exact expression (35), simulation, and approximate expression [26, Eq. (39)], for $k = 1$, QPSK modulation, $N_R = N_T = 4$, $K = 7$ dB, AS $= 51°$ (i.e., WINNER II scenario A1 averages).

averaged over all streams [26, Figs. 4, 5] [29, Fig. 2]. For the Rician–Rayleigh case discussed herein, other (unshown) numerical results have further revealed that decreasing K yields an increasing AEP gap for different AS values. This is expected because, for $K \to 0$, Rician–Rayleigh fading approaches Rayleigh–Rayleigh fading. It is nevertheless interesting that, for WINNER II-like values of K, the transmit AS (i.e., correlation) does not affect ZF performance for the Rician-fading stream.

Fig. 4 shows the AEP from the exact expression (35) and simulation vs. the Rician K factor, for $\gamma_b = 10$ dB, and $N_T = 1 : 4$. The AEP decreases with increasing K until it reaches a floor (not shown for $N_T = 1$, because it is very low). This figure reveals that performance can degrade dramatically for the Rician stream even at high K with more interfering Rayleigh streams, due to diminishing diversity order N, which is relevant in femtocells that experience interference. McKay *et al.* [15, Fig. 3] have revealed similar issues for MIMO optimum combining.

Fig. 5 depicts the amount of fading from Table I for the feasible AS range and several relevant values of K. Note that higher K yields lower amount of fading, as expected. Also, for higher

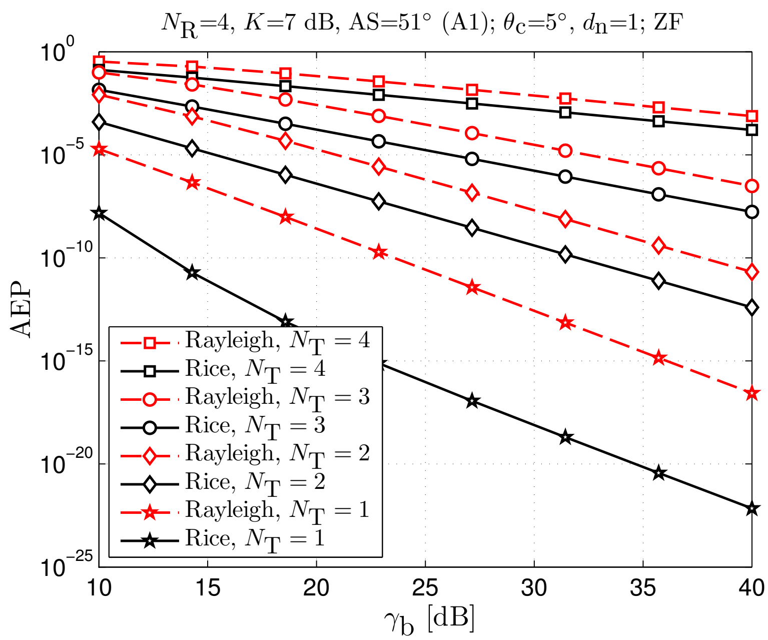

Fig. 2. AEP from exact expression (35), for Rician fading and Rayleigh fading, for $k = 1$, QPSK modulation, $N_{\mathrm{R}} = 4$, $N_{\mathrm{T}} = 1:4$, $K = 7$ dB, AS $= 51°$.

K, the amount of fading varies less with the AS, which corroborates the observation that AS does not affect the AEP made earlier based on results shown for the Rician case in Fig. 3.

Fig. 6 shows the p.d.f. of γ_1 (in linear units) from the exact expression (26) and from simulation, for $N_{\mathrm{T}} = 3$, $N_{\mathrm{R}} = 4$, AS $= 51°$, $K = 0$ dB, and $\gamma_{\mathrm{b}} = 5.2$ dB. For the same settings, Fig. 7 shows the outage probability vs. γ_{b}, from the exact expression (38) and from simulation. The threshold SNR γ_{th} has been set to 8.2 dB, which corresponds for QPSK to the relevant error probability value $P_{\mathrm{e,th}} = 10^{-2}$ [56]. These figures again reveal a close match between our analysis and simulations. The P_{o} plot also confirms a diversity order of N for both Rician and Rayleigh fading, with the former displaying an additional array gain.

VI. Summary and Conclusions

This work has derived exact expressions for performance measures of spatial multiplexing with ZF detection in Rician–Rayleigh fading. Instead of relying on the Wishart distribution in the SNR analysis, we have exploited the SNR expressed as a Hermitian form to derive its m.g.f. Thus, we have revealed that the ZF SNR distribution is an infinite linear combination

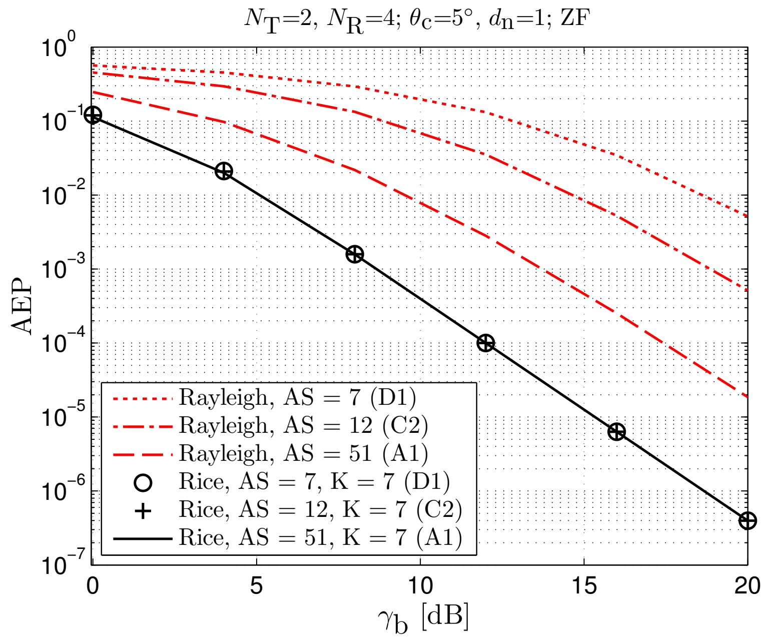

Fig. 3. AEP from exact expression (35), for $k = 1$, QPSK modulation, $N_R = 4$, $N_T = 2$, and AS (°) and K (dB) set to averages for WINNER II scenarios A1, C2, and D1.

of Gamma distributions with simple coefficients. From the derived ZF SNR m.g.f., p.d.f., and c.d.f. expressions, we have expressed the SNR moments, as well as the ZF diversity order, average error probability, outage probability, and average capacity. Numerical results have validated our analysis against Monte Carlo simulations, and have offered new insights into effects of channel fading parameters on ZF performance for Rician–Rayleigh fading. Thus, we have learned that symbol-detection performance for the ZF-detected Rician stream is: 1) not affected by the 'direction' of the mean of its channel vector; 2) largely unaffected by transmit correlation, at realistic K values; 3) dramatically degraded by more Rayleigh interferers, even for large K, which is relevant for femtocells.

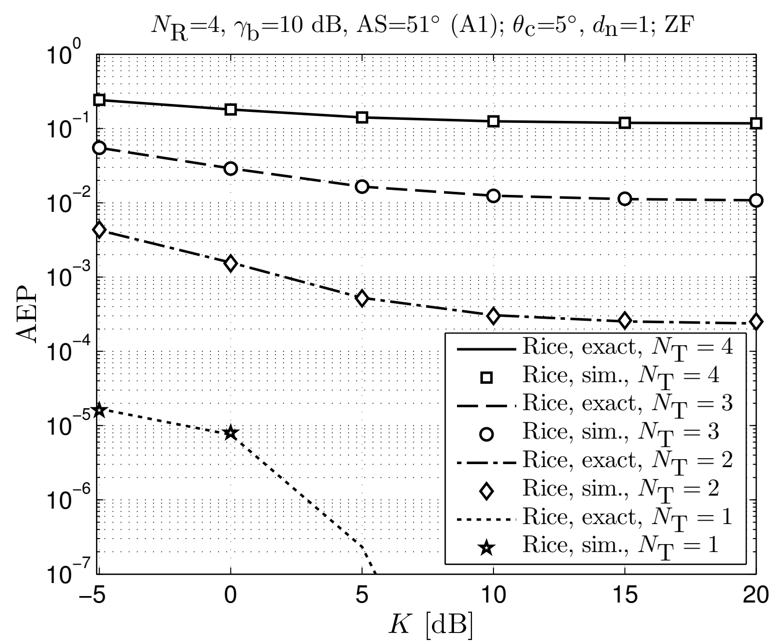

Fig. 4. AEP vs. K from the exact expression (35) and from simulation, for $k = 1$, QPSK modulation, $N_{\rm R} = 4$, $N_{\rm T} = 1:4$, AS $= 51^\circ$, $K = 0$ dB, $\gamma_{\rm b} = 10$ dB.

Appendix A
Derivation of γ_1 Conditioned on $\widetilde{\mathbf{H}}$ (i.e., $\mathbf{Q}$)

The derivation shown below follows closely that from [20, Section 3], but we provide it for completeness. We partition the $N_{\rm T} \times N_{\rm T}$ transmit correlation matrix $\mathbf{R}_{{\rm T},K}$ according to (6) as

$$\mathbf{R}_{{\rm T},K} = \begin{bmatrix} \mathbf{R}_{{\rm T},K_{11}} & \mathbf{R}_{{\rm T},K_{12}} \\ \mathbf{R}_{{\rm T},K_{21}} & \mathbf{R}_{{\rm T},K_{22}} \end{bmatrix}, \tag{41}$$

where $\mathbf{R}_{{\rm T},K_{22}}$ is a $(N_{\rm T}-1)\times(N_{\rm T}-1)$ matrix and $\mathbf{R}_{{\rm T},K_{11}}$ is a scalar. It can then be shown that [20, Appendix] [58, Section 9.11.3, §2.b]

$$\left[\mathbf{R}_{{\rm T},K}^{-1}\right]_{1,1} = 1/\left(\mathbf{R}_{{\rm T},K_{11}} - \mathbf{R}_{{\rm T},K_{12}}\,\mathbf{R}_{{\rm T},K_{22}}^{-1}\,\mathbf{R}_{{\rm T},K_{21}}\right), \tag{42}$$

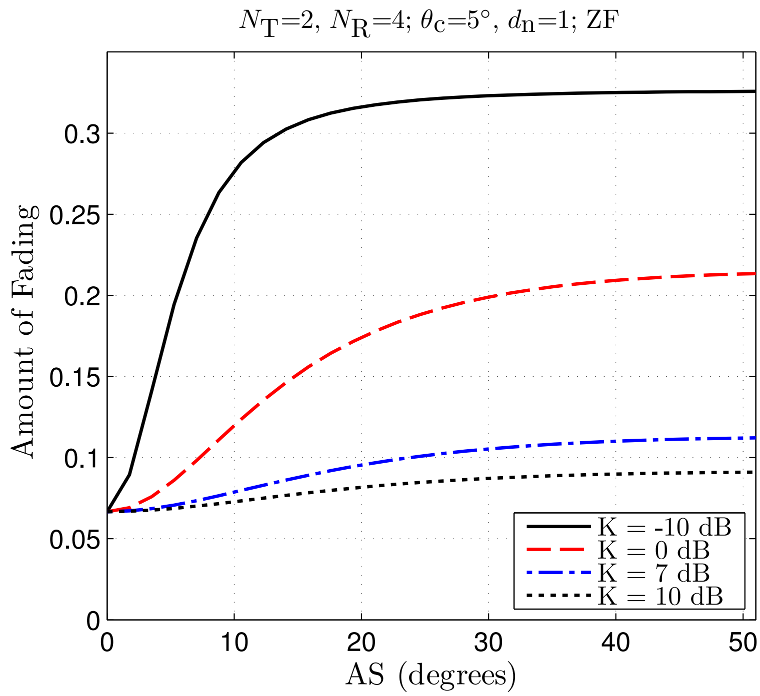

Fig. 5. Amount of fading from expression in Table I vs. AS, for $k = 1$, $N_{\mathrm{R}} = 4$, $N_{\mathrm{T}} = 2$, and $K = -10, 0, 7, 10$ dB.

which is needed below and in the main text. Now, since the elements of $\mathbf{h}_1$ and $\widetilde{\mathbf{H}}$ in (6) are jointly Gaussian, the distribution of $\mathbf{h}_1$ given $\widetilde{\mathbf{H}}$ is [20, Appendix]

$$\mathbf{h}_1|\widetilde{\mathbf{H}} \sim \mathcal{N}_{\mathrm{c}}\left(\mathbf{h}_{1,\mathrm{d}} + \left[\widetilde{\mathbf{H}} - \widetilde{\mathbf{H}}_{\mathrm{d}}\right]\underbrace{\mathbf{R}_{\mathrm{T},K_{22}}^{-1}\mathbf{R}_{\mathrm{T},K_{21}}}_{=\mathbf{a}}, \mathbf{I}_{N_{\mathrm{R}}} \otimes \frac{1}{\left[\mathbf{R}_{\mathrm{T},K}^{-1}\right]_{1,1}}\right) \tag{43}$$

$$\sim \mathcal{N}_{\mathrm{c}}\left(\underbrace{\left[\mathbf{h}_{1,\mathrm{d}} - \widetilde{\mathbf{H}}_{\mathrm{d}}\mathbf{a}\right]}_{=\boldsymbol{\mu}} + \widetilde{\mathbf{H}}\mathbf{a}, \frac{1}{\left[\mathbf{R}_{\mathrm{T},K}^{-1}\right]_{1,1}}\mathbf{I}_{N_{\mathrm{R}}}\right), \tag{44}$$

where $\mathbf{a}$ and $\boldsymbol{\mu}$ are deterministic vectors of dimensions $(N_{\mathrm{T}} - 1) \times 1$ and $N_{\mathrm{R}} \times 1$, respectively. As in [20, Section 3], defining the random vector

$$\mathbf{x} \sim \mathcal{N}_{\mathrm{c}}\left(\boldsymbol{\mu}, \frac{1}{\left[\mathbf{R}_{\mathrm{T},K}^{-1}\right]_{1,1}}\mathbf{I}_{N_{\mathrm{R}}}\right), \tag{45}$$

and substituting it in (44) yields

$$\mathbf{h}_1|\widetilde{\mathbf{H}} \simeq \mathbf{x} + \widetilde{\mathbf{H}}\mathbf{a} \sim \mathcal{N}_{\mathrm{c}}\left(\boldsymbol{\mu} + \widetilde{\mathbf{H}}\mathbf{a}, \frac{1}{\left[\mathbf{R}_{\mathrm{T},K}^{-1}\right]_{1,1}}\mathbf{I}_{N_{\mathrm{R}}}\right). \tag{46}$$

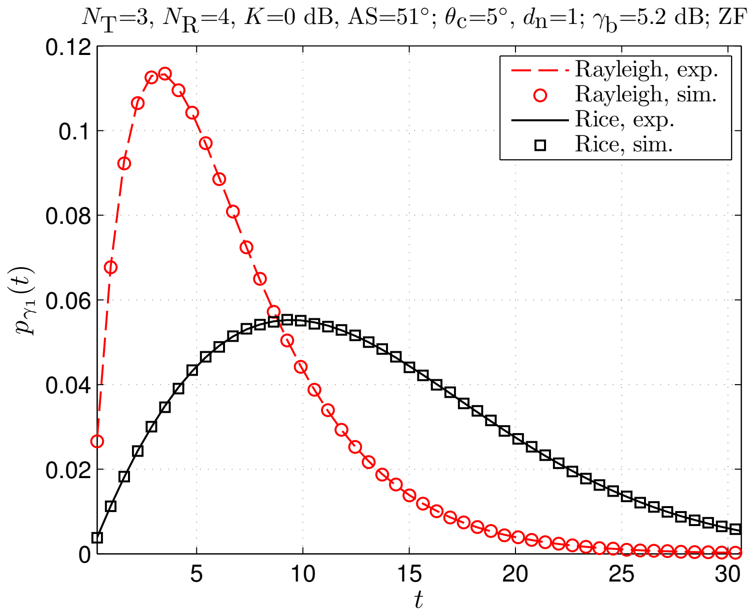

Fig. 6. P.d.f. of γ_1 (in linear units) from exact expression (26) and from simulation, for $N_R = 4$, $N_T = 3$, AS $= 51°$, $K = 0$ dB, $\gamma_b = 5.2$ dB.

Thus, the receive-correlation remains zero after conditioning on $\widetilde{\mathbf{H}}$. On the other hand, the transmit-correlation enters the distribution of $\mathbf{h}_1|\widetilde{\mathbf{H}}$ through $\mathbf{a} = \mathbf{R}_{\mathrm{T},K_{22}}^{-1}\mathbf{R}_{\mathrm{T},K_{21}}$ and $\left[\mathbf{R}_{\mathrm{T},K}^{-1}\right]_{1,1}$. Now, substituting (46) in (7) and further manipulating as in [20, Eqs. (11),(12)] yields

$$\begin{aligned}\gamma_1|\widetilde{\mathbf{H}} &\simeq \frac{E_s}{N_0}\frac{1}{N_T}\left(\mathbf{x}+\widetilde{\mathbf{H}}\mathbf{a}\right)^{\mathcal{H}}\left[\mathbf{I}_{N_R}-\widetilde{\mathbf{H}}\left(\widetilde{\mathbf{H}}^{\mathcal{H}}\widetilde{\mathbf{H}}\right)^{-1}\widetilde{\mathbf{H}}^{\mathcal{H}}\right]\left(\mathbf{x}+\widetilde{\mathbf{H}}\mathbf{a}\right)\\ &= \frac{E_s}{N_0}\frac{1}{N_T}\mathbf{x}^{\mathcal{H}}\left[\mathbf{I}_{N_R}-\widetilde{\mathbf{H}}\left(\widetilde{\mathbf{H}}^{\mathcal{H}}\widetilde{\mathbf{H}}\right)^{-1}\widetilde{\mathbf{H}}^{\mathcal{H}}\right]\mathbf{x} = \frac{E_s}{N_0}\frac{1}{N_T}\mathbf{x}^{\mathcal{H}}\mathbf{Q}\mathbf{x} = \gamma_1|\mathbf{Q}, \qquad (47)\end{aligned}$$

which can be written more conveniently as shown in the main text at page 9, Eqs. (10)-(12).

Notice that, although (47) has removed the explicit dependence of γ_1 on $\mathbf{a}$, an implicit dependence would remain, through the mean of $\mathbf{x}$, i.e., $\boldsymbol{\mu} = \mathbf{h}_{1,d} - \widetilde{\mathbf{H}}_d\mathbf{a}$. However, our main-text assumption $\widetilde{\mathbf{H}}_d = \mathbf{0}$ yields $\boldsymbol{\mu} = \mathbf{h}_{1,d}$, which removes also the implicit dependence. Thus, the transmit-correlation $\mathbf{R}_T$ affects the ZF SNR only through scalar $\left[\mathbf{R}_{\mathrm{T},K}^{-1}\right]_{1,1}$.

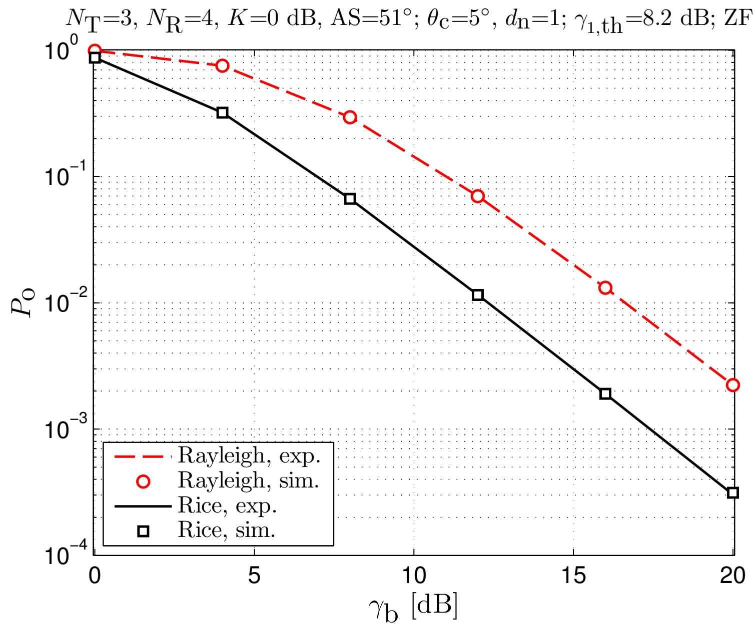

Fig. 7. Outage probability from exact expression (38) and from simulation, for $k = 1$, QPSK modulation, $N_{\rm R} = 4$, $N_{\rm T} = 3$, AS $= 51^\circ$, $K = 0$ dB, and $\gamma_{\rm th} = 8.2$ dB.

APPENDIX B
SPECIAL CASES, PERFORMANCE RELATIONSHIPS

A. SIMO MRC in Uncorrelated Rician Fading

For SIMO, i.e., when the single transmitted stream[8] is received with $N_{\rm R}$ antennas, ZF reduces to MRC. As throughout this work, we assume receive-uncorrelated fading. The fading is herein also assumed to be Rician. Since in this case $N_{\rm T} = 1$, we have $N = N_{\rm R}$ and then (22) yields ${}_1F_1\left(N_{\rm R}; N_{\rm R}; \sigma\right) = e^{\sigma}$ [42, Eq. (9.35)]. Further, matrix $\mathbf{R}_{\rm T}$ reduces to the unit scalar, α from (14) reduces to $KN_{\rm R}$, and Γ_1 from (11) reduces to $\frac{E_{\rm s}}{N_0}\frac{1}{K+1}$. Thus, the m.g.f. for the MRC SNR in uncorrelated Rician fading reduces from (23) to:

$$M_{\gamma_1,\text{MRC,Rice}}(s) = \frac{1}{\left(1-\Gamma_1 s\right)^{N_{\rm R}}} \exp\left\{KN_{\rm R}\frac{\Gamma_1 s}{1-\Gamma_1 s}\right\}. \tag{48}$$

The following corresponding AEP expression is obtained by substituting (48) into (34):

$$P_{\text{e,1,MRC,Rice}} = \frac{1}{\pi}\int_0^{\frac{M-1}{M}\pi}\left[\left(\frac{\sin^2\theta}{\sin^2\theta + \Gamma_1\sin^2\frac{\pi}{M}}\right)\exp\left\{-K\frac{\Gamma_1\sin^2\frac{\pi}{M}}{\sin^2\theta+\Gamma_1\sin^2\frac{\pi}{M}}\right\}\right]^{N_{\rm R}} d\theta. \tag{49}$$

[8]For notational consistency, the stream index is maintained for SIMO, even though a single stream is transmitted.

The SNR m.g.f. and AEP expressions we previously derived for SIMO MRC and correlated Rician fading in [59, Eqs. (22), (26)] reduce for uncorrelated fading to (48), and (49).

B. MIMO ZF vs. SIMO MRC Performance in Rayleigh and Rician Fading

For MIMO, let us now also assume zero transmit-correlation, i.e., $\mathbf{R}_{\mathrm{T}} = \mathbf{I}_{N_{\mathrm{T}}}$, and Rayleigh fading. Then, in the MIMO ZF SNR m.g.f. expression (27), $\Gamma_1 = \frac{E_{\mathrm{s}}}{N_0}\frac{1}{N_{\mathrm{T}}}$ accounts for the fact that energy $\frac{E_{\mathrm{s}}}{N_{\mathrm{T}}}$ is spent for each of the N_{T} transmitted symbols, so that energy E_{s} is spent during each symbol interval. On the other hand, for SIMO MRC in Rayleigh fading, (27) for $N_{\mathrm{T}} = 1$ or (48) for $K = 0$ yield the SNR m.g.f. expression

$$M_{\gamma_1,\mathrm{MRC,Rayleigh}}(s) = \frac{1}{(1-\Gamma_1 s)^{N_{\mathrm{R}}}}, \tag{50}$$

whereby $\Gamma_1 = \frac{E_{\mathrm{s}}}{N_0}$ reflects the fact that the entire energy E_{s} is transmitted in a single symbol. Thus, comparing the SNR m.g.f. expressions for MIMO ZF from (27) and for SIMO MRC from (50) reveals performance equivalence when $E_{\mathrm{s,MRC}} = E_{\mathrm{s,ZF}}/N_{\mathrm{T,ZF}}$, and $N_{\mathrm{R,MRC}} = N_{\mathrm{ZF}} = N_{\mathrm{R,ZF}} - N_{\mathrm{T,ZF}} + 1$, for uncorrelated Rayleigh fading[9]. However, (23) and (48) do not support an analogous performance relationship between MIMO ZF and SIMO MRC for Rician fading.

C. Per-Stream Performance for MIMO ZF in Rayleigh and Rician Fading

For MIMO ZF in Rayleigh–Rayleigh fading (i.e., $K = 0$) that is receive-uncorrelated, the SNR m.g.f. for stream 1 is expressed in (27). The SNR m.g.f. for any other stream can be expressed analogously, i.e., the SNR for stream k is Gamma distributed with shape parameter N and scale parameter [19] [20]:

$$\Gamma_k = \frac{E_{\mathrm{s}}}{N_0}\frac{1}{N_{\mathrm{T}}}\frac{1}{\left[\mathbf{R}_{\mathrm{T},K}^{-1}\right]_{k,k}}. \tag{51}$$

Thus, for Rayleigh fading, ZF AEP performance for any stream $k = 2 : N_{\mathrm{T}}$ is described by the same expression as for stream 1, i.e., Eq. (37), simply by replacing Γ_1 with Γ_k. A similar analogy is not possible for Rician–Rayleigh fading because, whereas the exact SNR m.g.f. for the Rician stream is given by (23), that for the Rayleigh streams is unknown[10].

[9]This is not surprising because, by definition, spatial multiplexing transmits multiple symbols whereas ZF cancels the interference and provides diversity gain.

[10]Nevertheless, for the Rayleigh streams, the SNR m.g.f. derived by approximating the Wishart distribution as described in [26] has been found satisfactorily accurate (through unshown numerical results).

References

[1] T. L. Marzetta and B. M. Hochwald, "Capacity of a mobile multiple-antenna communication link in Rayleigh flat fading," *IEEE Transactions on Information Theory,*, vol. 45, no. 1, pp. 139–157, Jan. 1999.

[2] A. J. Paulraj, R. U. Nabar, and D. A. Gore, *Introduction to Space-Time Wireless Communications*. Cambridge, UK: Cambridge University Press, 2003.

[3] M. K. Simon and M.-S. Alouini, *Digital Communication Over Fading Channels*, 2nd ed. Hoboken, New Jersey, USA: John Wiley and Sons, 2005.

[4] D. Gesbert, M. Kountouris, R. W. Heath, C.-B. Chae, and T. Salzer, "Shifting the MIMO paradigm," *IEEE Signal Processing Magazine*, vol. 24, no. 5, pp. 36–46, 2007.

[5] J. Lee, J. Han, and J. Zhang, "MIMO technologies in 3GPP LTE and LTE-Advanced," *EURASIP Journal on Wireless Communications and Networking*, vol. 2009.

[6] K. Nishimori, R. Kudo, N. Honma, Y. Takatori, and M. Mizoguchi, "16x16 multiuser MIMO testbed employing simple adaptive modulation scheme," in *IEEE Vehicular Technology Conference (VTC Spring)*, April 2010, pp. 1–5.

[7] O. Nasr, O. Takeshita, W. Zhu, and B. Daneshrad, "Field trial results of a 4x4 MIMO–OFDM real time testbed," in *IEEE International Conference on Communications (ICC'10)*, May 2010, pp. 1–5.

[8] K. Werner, H. Asplund, D. Figueiredo, N. Jalden, and B. Halvarsson, "LTE-advanced 8×8 MIMO measurements in an indoor scenario," in *International Symposium on Antennas and Propagation (ISAP'12)*, Nov. 2012, pp. 750–753.

[9] G. Hiertz, D. Denteneer, L. Stibor, Y. Zang, X. Costa, and B. Walke, "The IEEE 802.11 universe," *IEEE Communications Magazine*, vol. 48, no. 1, pp. 62–70, January 2010.

[10] Q. Li, G. Li, W. Lee, M. Lee, D. Mazzarese, B. Clerckx, and Z. Li, "MIMO techniques in WiMAX and LTE: a feature overview," *IEEE Communications Magazine*, vol. 48, no. 5, pp. 86–92, May 2010.

[11] A. Ghosh, R. Ratasuk, B. Mondal, N. Mangalvedhe, and T. Thomas, "LTE-advanced: next-generation wireless broadband technology," *IEEE Wireless Communications*, vol. 17, no. 3, pp. 10–22, June 2010.

[12] X. Ma and W. Zhang, "Fundamental limits of linear equalizers: diversity, capacity, and complexity," *IEEE Transactions on Information Theory*, vol. 54, no. 8, pp. 3442–3456, 2008.

[13] R. Louie, M. Mckay, and I. Collings, "New performance results for multiuser optimum combining in the presence of Rician fading," *IEEE Transactions on Communications*, vol. 57, no. 8, pp. 2348–2358, Aug. 2009.

[14] N. Kim, Y. Lee, and H. Park, "Performance analysis of MIMO system with linear MMSE receiver," *IEEE Transactions on Wireless Communications*, vol. 7, no. 11, pp. 4474–4478, 2008.

[15] M. McKay, A. Zanella, I. Collings, and M. Chiani, "Error probability and SINR analysis of optimum combining in Rician fading," *IEEE Transactions on Communications*, vol. 57, no. 3, pp. 676–687, March 2009.

[16] P. Liu and I.-M. Kim, "Exact and closed-form error performance analysis for hard MMSE-SIC detection in MIMO systems," *IEEE Transactions on Communications*, vol. 59, no. 9, pp. 2463–2477, 2011.

[17] Y. Jiang, M. Varanasi, and J. Li, "Performance analysis of ZF and MMSE equalizers for MIMO systems: An in-depth study of the high SNR regime," *IEEE Transactions on Information Theory*, vol. 57, no. 4, pp. 2008–2026, April 2011.

[18] F. A. T. B. N. Monteiro, "Lattices in MIMO spatial multiplexing: Detection and geometry," Ph.D. dissertation, University of Cambridge, 2012.

[19] D. A. Gore, R. W. Heath Jr, and A. J. Paulraj, "Transmit selection in spatial multiplexing systems," *IEEE Communications Letters*, vol. 6, no. 11, pp. 491–493, 2002.

[20] M. Kiessling and J. Speidel, "Analytical performance of MIMO zero-forcing receivers in correlated Rayleigh fading environments," in *IEEE Workshop on Signal Processing Advances in Wireless Communications (SPAWC'03)*, June 2003, pp. 383–387.

[21] C. Wang, E. K. S. Au, R. D. Murch, W. H. Mow, R. S. Cheng, and V. Lau, "On the performance of the MIMO zero-forcing receiver in the presence of channel estimation error," *IEEE Transactions on Wireless Communications*, vol. 6, no. 3, pp. 805–810, Mar. 2007.

[22] K. Nobandegani and P. Azmi, "Effects of inaccurate training-based minimum mean square error channel estimation on the performance of multiple input-multiple output vertical Bell Laboratories space-time zero-forcing receivers," *IET Communications*, vol. 4, no. 6, pp. 663–674, April 2010.

[23] ——, "A study of the extreme effects of fading correlation and the impact of imperfect MMSE channel estimation on the performance of SIMO zero-forcing receivers and on the capacity-maximizing strategy in SIMO links," *IEEE Transactions on Vehicular Technology*, vol. 59, no. 3, pp. 1294–1306, March 2010.

[24] P. Kyosti, J. Meinila, L. Hentila, and *et al.*, "WINNER II Channel Models. Part I," CEC, Tech. Rep. IST-4-027756, 2008.

[25] C.-X. Wang, X. Hong, X. Ge, X. Cheng, G. Zhang, and J. Thompson, "Cooperative MIMO channel models: A survey," *IEEE Communications Magazine*, vol. 48, no. 2, pp. 80–87, Feb. 2010.

[26] C. Siriteanu, Y. Miyanaga, S. D. Blostein, S. Kuriki, and X. Shi, "MIMO zero-forcing detection analysis for correlated and estimated Rician fading," *IEEE Transactions on Vehicular Technology*, vol. 61, no. 7, pp. 3087–3099, September 2012.

[27] H. Omote, Y. Sugita, Y. Ohta, and T. Fujii, "Carrier frequency characteristic of time-spatial profile in outdoor LOS environments," in *Vehicular Technology Conference (VTC'12-Spring)*, 2012, pp. 1–5.

[28] R. Xu and F. C. M. Lau, "Performance analysis for MIMO systems using zero forcing detector over fading channels," *IEE Proc. Communications*, vol. 153, no. 1,2, pp. 74–80, February 2006.

[29] H. A. A. Saleh and W. Hamouda, "Performance of zero-forcing detectors over MIMO flat-correlated Ricean fading channels," *IET Communications*, vol. 3, no. 1, pp. 10–16, January 2009.

[30] W. Wang, G. Shen, S. Jin, D. Wang, and J. Chen, "Approximate minimum SER precoding for spatial multiplexing over Ricean channels," in *IEEE 20th International Symposium on Personal, Indoor and Mobile Radio Communications, (PIMRC'09)*, Sept. 2009, pp. 2360–2364.

[31] H. S. Steyn and J. J. J. Roux, "Approximations for the non-central Wishart distributions," *South African Statistical Journal*, vol. 6, pp. 164–173, 1972.

[32] C. Chayawan and V. A. Aalo, "On the outage probability of optimum combining and maximal ratio combining schemes in an interference-limited Rice fading channel," *IEEE Transactions on Communications*, vol. 50, no. 4, pp. 532–535, 2002.

[33] M. Kang, M.-S. Alouini, and L. Yang, "Outage probability and spectrum efficiency of cellular mobile radio systems with smart antennas," *IEEE Transactions on Communications*, vol. 50, no. 12, pp. 1871–1877, 2002.

[34] H. Claussen, L. T. Ho, and L. G. Samuel, "An overview of the femtocell concept," *Bell Labs Technical Journal*, vol. 13, no. 1, pp. 221–245, 2008.

[35] J. Hoydis, M. Kobayashi, and M. Debbah, "Green small-cell networks," *IEEE Vehicular Technology Magazine*, vol. 6, no. 1, pp. 37–43, 2011.

[36] J. G. Andrews, H. Claussen, M. Dohler, S. Rangan, and M. C. Reed, "Femtocells: Past, present, and future," *IEEE Journal on Selected Areas in Communications*, vol. 30, no. 3, pp. 497–508, 2012.

[37] M. Yavuz, F. Meshkati, S. Nanda, A. Pokhariyal, N. Johnson, B. Raghothaman, and A. Richardson, "Interference

management and performance analysis of UMTS/HSPA+ femtocells," *IEEE Communications Magazine*, vol. 47, no. 9, pp. 102–109, Sep. 2009.

[38] Y. Jeong, H. Shin, and M. Win, "Interference rejection combining in two-tier femtocell networks," in *IEEE 22nd International Symposium on Personal Indoor and Mobile Radio Communications (PIMRC)*, 2011, pp. 137–141.

[39] N. Saquib, E. Hossain, L. B. Le, and D. I. Kim, "Interference management in OFDMA femtocell networks: issues and approaches," *Wireless Communications, IEEE*, vol. 19, no. 3, pp. 86–95, June 2012.

[40] T. Zahir, K. Arshad, A. Nakata, and K. Moessner, "Interference management in femtocells," *IEEE Communications Surveys Tutorials*, vol. 15, no. 1, pp. 293–311, 1st quarter 2013.

[41] D. Basnayaka, P. Smith, and P. Martin, "Exact dual-user macrodiversity performance with linear receivers in flat Rayleigh fading," in *IEEE International Conference on Communications (ICC)*, June 2012, pp. 4089–4094.

[42] L. C. Andrews, *Special functions for engineers and applied mathematicians*. NY, USA: MacMillan, 1985.

[43] D. Zwillinger and S. Kokoska, *CRC Standard Probability and Statistics Tables and Formulae. Student Edition.* Boca Raton, FL: Chapman and Hall/CRC, 2000.

[44] M. Abramowitz and I. A. Stegun, Eds., *Handbook of Mathematical Functions with Formulas, Graphs and Mathematical Tables*. New York, NY 10014: Dover Publications, Inc., 1995.

[45] R. G. Gallager, "Circularly-symmetric Gaussian random vectors," *preprint*, 2008.

[46] G. Taricco and G. Coluccia, "Optimum receiver design for correlated Rician fading MIMO channels with pilot-aided detection," *IEEE Journal on Selected Areas in Communications*, vol. 25, no. 7, pp. 1311–1321, Sept. 2007.

[47] O. Oteri, E. Yoon, and A. Paulraj, "Linear precoding for high-K-factor channels exploiting channel mean and covariance information," *IEEE Transactions on Vehicular Technology*, vol. 56, no. 5, pp. 2581–2589, Sept. 2007.

[48] S. Loyka and G. Levin, "On physically-based normalization of MIMO channel matrices," *IEEE Transactions on Wireless Communications*, vol. 8, no. 3, pp. 1107–1112, March 2009.

[49] C.-J. Chen and L.-C. Wang, "Performance analysis of scheduling in multiuser MIMO systems with zero-forcing receivers," *IEEE Journal on Selected Areas in Communications*, vol. 25, no. 7, pp. 1435–1445, Sept. 2007.

[50] R. I. Muirhead, *Aspects of Multivariate Statistical Theory*. Hoboken, New Jersey, USA: John Wiley and Sons, 2005.

[51] G. L. Turin, "The characteristic function of Hermitian quadratic forms in complex normal random variables," *Biometrika*, vol. 47, no. 1/2, pp. 199–201, June 1960.

[52] D. Love, J. Heath, R.W., and T. Strohmer, "Grassmannian beamforming for multiple-input multiple-output wireless systems," *IEEE Transactions on Information Theory*, vol. 49, no. 10, pp. 2735–2747, Oct. 2003.

[53] A. James, "Distributions of matrix variates and latent roots derived from normal samples," *The Annals of Mathematical Statistics*, pp. 475–501, 1964.

[54] N. L. Johnson, S. Kotz, and N. Balakrishnan, *Continuous Univariate Distributions*, 2nd ed. New York: John Wiley and Sons, Inc., 1993, vol. 1 and 2.

[55] Y. Dhungana and C. Tellambura, "New simple approximations for error probability and outage in fading," *IEEE Communications Letters*, vol. 16, no. 11, pp. 1760–1763, November 2012.

[56] C. Siriteanu and S. D. Blostein, "Performance and complexity analysis of eigencombining, statistical beamforming, and maximal-ratio combining," *IEEE Transactions on Vehicular Technology*, vol. 58, no. 7, pp. 3383–3395, September 2009.

[57] M. Alouini and A. Goldsmith, "Capacity of Rayleigh fading channels under different adaptive transmission and diversity-combining techniques," *IEEE Transactions on Vehicular Technology*, vol. 48, no. 4, pp. 1165–1181, 1999.

[58] H. Lutkepohl, *Handbook of Matrices*. New York, NY: John Wiley and Sons, 1996.

[59] C. Siriteanu, Y. Miyanaga, and S. D. Blostein, "Smart antenna performance and complexity for correlated azimuth spread and Rician K-factor," in *Int. Conf. on Green Circuits and Systems, Shanghai, China, (ICGCS'10)*, June 2010.